

Alzheimer PHF-tau aggregates do not spread tau pathology to the brain via the Retino-tectal projection after intraocular injection in male mouse models

M.-A. de Fisenne^a, Z. Yilmaz^a, R. De Decker^a, V. Suain^a, L. Buée^b, K. Ando^a, J.-P. Brion^a, K. Leroy^{a,*}

^a Laboratory of Histology, Neuroanatomy and Neuropathology, ULB Neuroscience Institute, Université Libre de Bruxelles, Faculty of Medicine, Brussels, Belgium

^b INSERM, U837. Université de Lille 2, Lille, France

ARTICLE INFO

Keywords:

Neurofibrillary tangles
Intraocular injection
Transgenic mouse
Alzheimer's disease
Retina
Tau pathology propagation

ABSTRACT

Neurofibrillary tangles (NFT), a neuronal lesion found in Alzheimer's disease (AD), are composed of fibrillary aggregates of modified forms of tau proteins. The propagation of NFT follows neuroanatomical pathways suggesting that synaptically connected neurons could transmit tau pathology by the recruitment of normal tau in a prion-like manner. Moreover, the intracerebral injection of pathological tau from AD brains induces the seeding of normal tau in mouse brain. Creutzfeldt-Jacob disease has been transmitted after ocular transplants of cornea or sclera and the scrapie agent can spread across the retino-tectal pathway after intraocular injection of scrapie mouse brain homogenates. In AD, a tau pathology has been detected in the retina. To investigate the potential risk of tau pathology transmission during eye surgery using AD tissue material, we have analysed the development of tau pathology in the visual pathway of mice models expressing murine tau, wild-type or mutant human tau after intraocular injection of pathological tau proteins from AD brains. Although these pathological tau proteins were internalized in retinal ganglion cells, they did not induce aggregation of endogenous tau nor propagation of a tau pathology in the retino-tectal pathway after a 6-month incubation period. These results suggest that retinal ganglion cells exhibit a resistance to develop a tau pathology, and that eye surgery is not a major iatrogenic risk of transmission of tau pathology, contrary to what has been observed for transmission of infectious prions in prion diseases.

1. Introduction

Alzheimer's disease (AD) is a neurodegenerative disease characterized by the presence of neuronal lesions called neurofibrillary tangles composed of abnormally phosphorylated and aggregated tau proteins. These aggregated tau proteins found in neurofibrillary tangles form abnormal filaments called paired helical filaments (PHF). The development of tau pathology in brain of Alzheimer's disease (AD) patients is graded into 6 stages according to the neuroanatomical localisation and the density of NFT (Braak and Braak, 1991). Interestingly, the formation of NFT in the brain is not random but follows neuroanatomical pathways suggesting that synaptically connected neurons could transmit tau pathology by transcellular transfer of abnormal tau. In vitro and in vivo studies have suggested that abnormal tau can recruit and seed the

formation of new tau aggregates by a "Prion-like" mechanism (Mudher et al., 2017). Previous studies have shown that the intracerebral injection of pathological tau proteins (PHF-tau proteins) from AD brains induces the seeding of normal murine and human tau in mouse brain indicating that pathological tau can recruit endogenous tau to adopt a pathological form (Clavaguera et al., 2013; Audouard et al., 2016; Vergara et al., 2019).

The scrapie agent can spread across the retino-tectal pathway along neuronal pathways via axons emerging from the retina after intraocular injection of terminally affected scrapie mouse brain homogenates (Fraser, 1982). Infectious prions have been found in the retina and optic nerve in Creutzfeldt-Jacob patients and this disease has been transmitted after ocular transplants of cornea or sclera (Duffy et al., 1974; Heckmann et al., 1997; Mehta and Franks, 2002; Head et al., 2003; Head

* Corresponding author at: Laboratory of Histology, Neuroanatomy and Neuropathology, Université Libre de Bruxelles, Faculty of Medicine, 808, route de Lennik, Bldg GE, CP620, 1070, Brussels, Belgium.

E-mail address: Karelle.leroy@ulb.be (K. Leroy).

<https://doi.org/10.1016/j.nbd.2022.105875>

Received 22 April 2022; Received in revised form 27 August 2022; Accepted 21 September 2022

Available online 22 September 2022

0969-9961/© 2022 The Authors. Published by Elsevier Inc. This is an open access article under the CC BY-NC-ND license (<http://creativecommons.org/licenses/by-nc-nd/4.0/>).

et al., 2005). In Alzheimer's disease, a tau pathology has been detected in the inner cell layer and in the inner and outer plexiform layers of the retina (Schön et al., 2012; Den Haan et al., 2018). Moreover, the presence of phosphorylated tau has been demonstrated in eye fluids suggesting that all eye tissues could be potentially contaminated by these tau proteins (Gijts et al., 2021; Romaus-Sanjurjo et al., 2022). However, it is not known if pathological tau could seed the aggregation of normal tau after optical surgery or graft. To investigate the ability of PHF-tau proteins from AD brains to seed murine or human tau and induce spreading of tau pathology in the brain after an ocular contamination, we have investigated the formation of tau pathology in the retina, the lateral geniculate nucleus and the superior colliculus after the injection of PHF-tau proteins from AD brains in the eye vitreous chamber of mice expressing murine or human tau.

2. Material and methods

2.1. Human brain tissue

Human brain tissue samples were taken at autopsy from a demented patient clinically diagnosed as having AD (60 years old, female, post-mortem delay of 24 h, NFT Braak stage VI and amyloid plaques Thal stage 4) or from a nondemented control subject (67 years old, male, post-mortem delay of 24 h). Tissue samples were fixed with formalin 10% and embedded in paraffin for neuropathological examination or were kept at -80°C . The neuropathological examination confirmed the presence of NFT and amyloid plaques in this AD case and their absence in the control case. This study on postmortem brain tissue was performed in compliance and following approval of the Ethical Committee of the Medical School of the Free University of Brussels.

2.2. Preparation of human sarkosyl-insoluble PHF-Tau fraction

Sarkosyl fractionation of human brain tissue was performed as previously described (Brion et al., 1991a; Vergara et al., 2019). 0.5 g of frozen frontal cortex from AD and control cases was homogenized in 10 volumes of ice-cold PHF-extraction buffer (10 mM Tris-HCl (pH 7.4), 0.8 M NaCl, 1 mM EDTA, 10% sucrose). The homogenate was centrifuged at 15,000 xg for 20 min at 4°C . N-lauroylsarcosine sodium salt (L-5125; Sigma-Aldrich) was added to the supernatant to reach a final concentration of 1% (w/v). The lysate was incubated at 4°C overnight with a mild agitation followed by an ultracentrifugation at 180,000 xg for 30 min at 4°C . The Sarkosyl soluble supernatant was removed and the Sarkosyl-insoluble pellet containing PHF was gently rinsed and re-suspended in 0.25 ml of PBS by vigorous pipetting. The protein concentration was determined by Bradford protein assay (Bio-Rad) and adjusted to 2 $\mu\text{g}/\mu\text{l}$ for the AD case or 1 $\mu\text{g}/\mu\text{l}$ for the control case. These Sarkosyl fractions were aliquoted and kept at -20°C . This study on postmortem brain tissue was performed in compliance and following approval of the Ethical Committee of the Medical School of the Free University of Brussels.

2.3. Negative staining of Tau filaments by transmission electron microscopy

The Sarkosyl-insoluble material was ultrastructurally characterized by transmission electron microscopy. This material was adsorbed on formvar-carbon-coated EM grids and negatively stained with potassium phosphotungstate as reported (Vergara et al., 2019) before observation with a Zeiss EM 809 T at 80 kV. The average length of sarkosyl insoluble filaments was measured on 200 filaments with ImageJ software.

2.4. Biosensor FRET cells

The biosensor cellular assay (FRET) used cultured cells expressing a tau repeat domain (RD) fused to CFP and a tau RD fused to YFP (Furman

et al., 2015). This bio-assay is based on the uptake of seeds into cells which induces aggregation of tau-CFP and tau-YFP, producing a FRET signal. Cells were plated at a density of 400,000 cells per well in a 6-well plate. Eighteen hours later, cells were transfected with liposomes preparation by combining Xtremegene HP transfection reagent (Roche) with sarkosyl fractions from CTL or AD brains in Optimem medium. Liposome preparation was incubated 20 min at room temperature before adding to cells. Cells were observed with a Zeiss Axioplan microscope twenty-four hours after transfection.

2.5. Western blotting

The protein assay was performed with the Bradford method (Biorad). Sarkosyl insoluble fractions were heated in Laemmli buffer at 100°C for 5 min and were analysed by western blotting with anti-total tau B19 and anti-phosphotau PHF-1 antibodies as previously described (Frederick et al., 2015; Vanden Dries et al., 2017). Fractions (5 $\mu\text{g}/\text{lane}$) were run in 10% Tris-glycine SDS-PAGE gels and transferred on nitrocellulose membranes. The nitrocellulose sheets were blocked in semifat dry milk (10% (w/v) in Tris-buffered saline) for 1 h at room temperature and they were incubated with primary antibodies overnight followed by anti-rabbit or anti-mouse immunoglobulins conjugated to peroxidase. Finally, the membranes were incubated in pico substrate (Pierce). The ECL signal was captured using a Fusion SOLO 4S system equipped with a DARQ-7 camera and the fusion-capt software (Vilber-Lourmat). Blot quantitation was performed with ImageJ software (NIH) and data normalization between blots was performed by placing a standard in each blot. The standard used is a brain homogenate of a Tg22 mouse.

2.6. Mouse lines

Tg22 mice (also referred to as THY-Tau22 mice) express a 1N4R human tau isoform mutated at positions G272V and P301S, under control of a Thy1 promoter, and display tau pathology in absence of motor dysfunction (Schindowski et al., 2006). Gallyas-positive neurofibrillary tangles appear in the cortex and the hippocampus at 6 months of age in these mice (Schindowski et al., 2006). Only male heterozygous Tg22 mice were used in this study and male littermates non-transgenic mice (pooled and named hereafter with C57BL/6 J wild-type mice) were also used in this study.

hTau mice express the six human tau isoforms, under tau promoter, in the absence of murine tau (Andorfer et al., 2003). Briefly, it was made by crossing two mice lines, 8c mice, that produce all human tau isoforms (Duff et al., 2000) and TauKO mice that do not express murine tau, by disrupting MAPT gene with a cDNA for enhanced green fluorescent protein (EGFP) inserted into exon one (Tucker et al., 2001). Only male heterozygous animals for the hTau transgene were used in this study and male littermates that do not carry the hTau transgene but are KO for murine tau and named TauKO were used as controls.

All mouse lines were maintained on a C57BL/6 genetic background. Mice were genotyped by PCR using previously described primers for human tau, murine tau and GFP on genomic DNA as reported (Andorfer et al., 2003; Schindowski et al., 2006; Ando et al., 2011). All mice were maintained on a 12 h light/dark cycle, with food and water ad libitum. All studies on animals were performed in compliance and following approval of the Ethical committee for the care and use of laboratory animals of the medical School of the Free University of Brussels.

2.7. Intravitreal injection

Animals were anesthetized with a solution of xylazine 2% (Rompun, Bayer) and ketamine (10% v/v) (Nimatek, Eurovet) in physiological serum by intraperitoneal injection (100 $\mu\text{l}/10\text{ g}$ of body weight, final dose, 10 mg/kg xylazine, and 75 mg/kg ketamine). One drop of oxybuprocaine chlorhydrate 0,4% (4 mg/ml) (Unicaïne, Théa) was applied to the mouse eye as a topical anesthetic before intravitreal injection.

Mice were injected into the eye posterior vitreous chamber under a stereomicroscope with a 33 gauge needle connected to a Hamilton microsyringue (Hamilton Bonaduz AG, Bonaduz, Switzerland).

Two micrograms of Sarkosyl-insoluble material from AD brain or one microgram from CTL brain was injected in a volume of 1 μ l which corresponded to 3,5 mg of AD or CTL brain tissues.

2 μ g of cholera toxin subunit B (ThermoFisher) was injected in a volume of 1 μ l in three WT mice as positive control to validate the injection method and to visualize the toxin along the visual pathway as previously described (Angelucci et al., 1996)

2.8. Stereotaxic injection

Six-month-old WT mice were deeply anesthetized with a solution of xylazine (2% v/v) (Rompun, Bayer) and ketamine (10% v/v) (Nimatek) in physiological saline by intraperitoneal injection (100 μ l/10 g of body weight), final dose 10 mg/kg xylazine and 100 mg/kg ketamine). Unilateral stereotaxic injections were performed using a stereotaxic apparatus (Kopf instruments, Tujunga, CA) in the left primary somatosensory cortex (rostro-caudal -1,46 mm; lateral +0,15 mm; depth - 0,10 mm) as previously described (Vergara et al., 2019). One microgram of Sarkosyl-insoluble material was injected in a volume of 1 μ l at the concentration of 1 μ g/ μ l at a speed of 0.1 μ l/min with a pump (kdScientific), using a 200 μ m diameter needle (ThermoFisher). The needle was gently removed 5 min after injection.

2.9. Antibodies

The tau antibody (DAKO, A0024) is a rabbit polyclonal antibody raised to human, mouse and rat tau proteins. The B19 antibody, used to detect PHF in AD sarkosyl fraction by western blotting (Fig. 2), is a rabbit polyclonal antibody raised to adult bovine tau proteins. This antibody reacts with adult and fetal tau isoforms in bovine, rat, mouse and human nervous tissue in a phosphorylation-independent-manner (Brion et al., 1991b; Leroy et al., 2000). The BR21 rabbit polyclonal antibody is specific for human tau (Ando et al., 2011). The mouse monoclonal antibodies AT8 (Thermo Fisher, MN1020) and PHF-1 (kindly provided by Drs. P. Davies and S. Greenberg, New York) recognize tau phosphorylated at Ser 202 and Thr205 (Goedert et al., 1995) and at Ser396 and Ser404 respectively (Otvos Jr et al., 1994). The mouse monoclonal MC1 antibody (generous gift from Dr. P. Davis) recognizes a conformational epitope requiring both an N-terminal and a C-terminal fragments of tau (Jicha et al., 1997). The antibody raised against the subunit B of cholera toxin is a polyclonal goat antibody purchased from Calbiochem (227040).

2.10. Histological staining and immunohistochemistry

Mice were sacrificed by cervical dislocation and a sample number has been given allowing blinded analysis concerning the type of treatments that mice received. Eyes, optic nerves and brains were fixed in 10% formalin for 24 h before embedding in paraffin. Tissue sections (7 μ m thick) and immunohistochemical labellings were performed using the ABC method as previously described (Stygelbout et al., 2014). Briefly, tissue sections were treated with H₂O₂ to inhibit endogenous peroxidase and incubated with the blocking solution (10% normal horse serum in TBS). After an overnight incubation with the diluted primary antibody, the sections were sequentially incubated with either horse anti-mouse or goat anti-rabbit antibodies conjugated to biotin (Vector Laboratories) followed by the ABC complex (Vector Laboratories). The peroxidase activity was developed using diaminobenzidine (DAB) as chromogen. Slides were counterstained with hematoxylin and examined with a Zeiss Axioplan microscope. Digital images were acquired using an AxioCam HRc camera (Zeiss) and the Axiovision software (Zeiss).

2.11. Quantification of tau pathology

After immunolabelling with the AT8, PHF-1 and MC1 antibodies, the density of phospho-tau positive neurons in the lateral geniculate nucleus and in the superior colliculus was estimated in mice injected with AD or CTL fractions. Three adjacent sections were used per brain sample. The Stereo Investigator system software from MBF Bioscience associated to the AxioImager microscope (Zeiss) were used to perform automatically and systematic analyses of the entire geniculate or superior colliculus areas. The surface of the lateral geniculate nucleus or of the superior colliculus was measured on each section with the software and phospho-tau positive neurons were manually tagged. As a result, we calculated a density of phospho-tau positive neurons expressed as a number of positive neurons/mm².

2.12. Statistical analysis

Statistical analysis was performed using the Prism program version 5.0 (Graphpad Software, San Diego, CA). Statistical comparisons were performed using (two-tailed) Mann-Whitney test to compare two groups. Values of $p < 0.05$ were considered significant. Numbers of samples are indicated in the figure legends and ranges represent means \pm SD.

3. Results

3.1. Localisation and expression of tau in the retina

In this study, experiments have been done in mice that express murine tau (non-transgenic wild-type (WT) mice), human WT tau (hTau mice), human mutant tau and murine tau (Tg22 mice) or mice deficient in tau proteins (TauKO mice). To evaluate the distribution of tau proteins in the retina of these different mice models, an immunolabelling with anti-total tau or anti-human tau antibodies was performed on the retina of WT (Fig. 1 A and I), hTau (Fig. 1 B and J), Tg22 (Fig. 1 C and K) and TauKO mice (Fig. 1 D and L). Total tau antibody detected tau proteins in the ganglion cell layer, in the inner plexiform layer, in the inner nuclear layer and in the outer plexiform layer of WT (Fig. 1 A), hTau (Fig. 1 B) and Tg22 (Fig. 1 C) mice retina. Human tau proteins were detected in the ganglion cell layer, in the inner and outer plexiform layers of hTau mice retina (Fig. 1 J). Tau proteins are expressed under the human tau promoter in this model. In Tg22 mice retina (Fig. 1 K), human tau proteins, expressed the Thy1.2 promoter, were only present in the ganglion cell layer. Moreover, human tau proteins were detected in the cell bodies of ganglion cells (small insets in Fig. 1 J and K). However, by Western blot analysis tau expression was found to be quite significantly lower in the retina compared to the brain in the different mouse models (total tau (WT: $p = 0.0022$; hTau: $p = 0.0079$ and Tg22: $p = 0.0022$) and human tau (hTau: $p = 0.0079$ and Tg22: $p = 0.0043$)) (Fig. 1 Q, R and S), e.g. being up to 10 times lower in the eye compared to the brain in WT mice. Human tau proteins were not detected in WT mice retina or brain (Fig. 1 I, M Q and S) and were never detected with anti-tau antibodies in the retina of TauKO mice as expected (Fig. 1 D, L and Q).

3.2. Characterisation of human Alzheimer sarkosyl fractions and seeding abilities

Before the intraocular injection, we have characterized sarkosyl fractions isolated from non-demented (named control (CTL)) or AD brains for the presence of tau proteins and the seeding abilities of these fractions in cultured cells or after stereotaxic injection in the brain (as positive controls) (Fig. 2). Phosphorylated tau proteins were detected with total or PHF-1 antibodies by western blotting in AD sarkosyl fraction (PHF-tau proteins) but were absent in CTL sarkosyl fractions (Fig. 2 A). The presence of tau filaments in the form of PHF in sarkosyl fractions

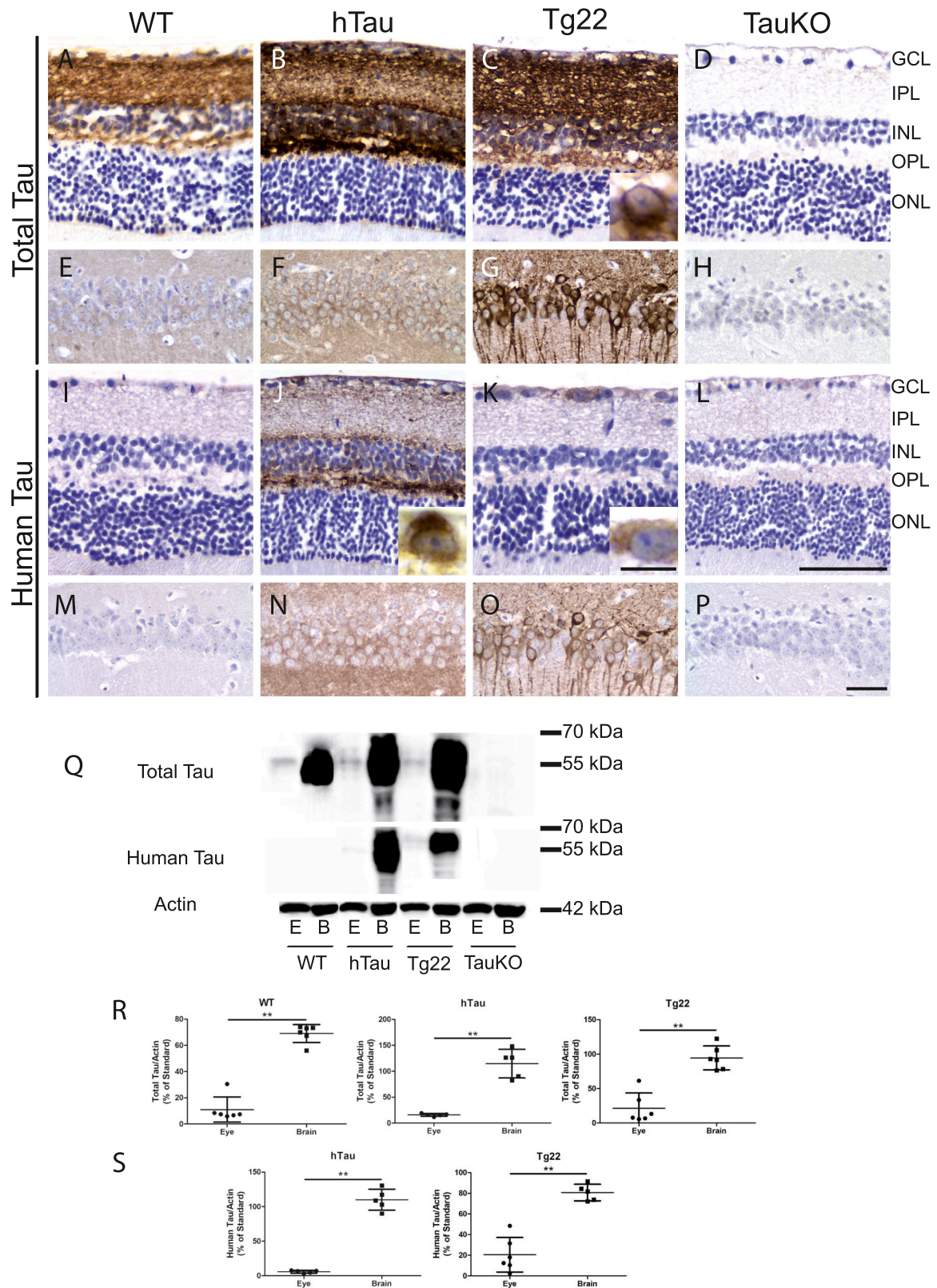


Fig. 1. Localization and expression of tau proteins in the retina of different mouse models. A-P: Immunolabelling with anti-total tau antibody (A-H) or with anti-human tau antibody (I-P) on the retina (A-D and I-L) or the hippocampus (E-H and M-P) of WT (A, E, I, M), hTau (B, F, J, N), Tg22 (C, G, K, O) and TauKO mice (D, H, L, P). Scale bars: L and P: 50 μ m, small window in K: 10 μ m.

Q: Western blotting of retina or brain homogenates of WT, hTau, Tg22 and TauKO mice with anti-total or anti-human tau antibodies. Actin was used as a control of charge.

R and S: Quantification of the expression of total tau (R) or human tau (S) proteins in retina and brain homogenates of WT, hTau and Tg22 mice. The results are presented as a percentage of the standard (which is 100%). The level of tau expression is significantly higher in brains compared to retinas in the different mice models (WT ($n = 6$), hTau ($n = 5$) and Tg22 ($n = 6$)). Two-tailed Mann-Whitney test, ** = $p < 0.01$.

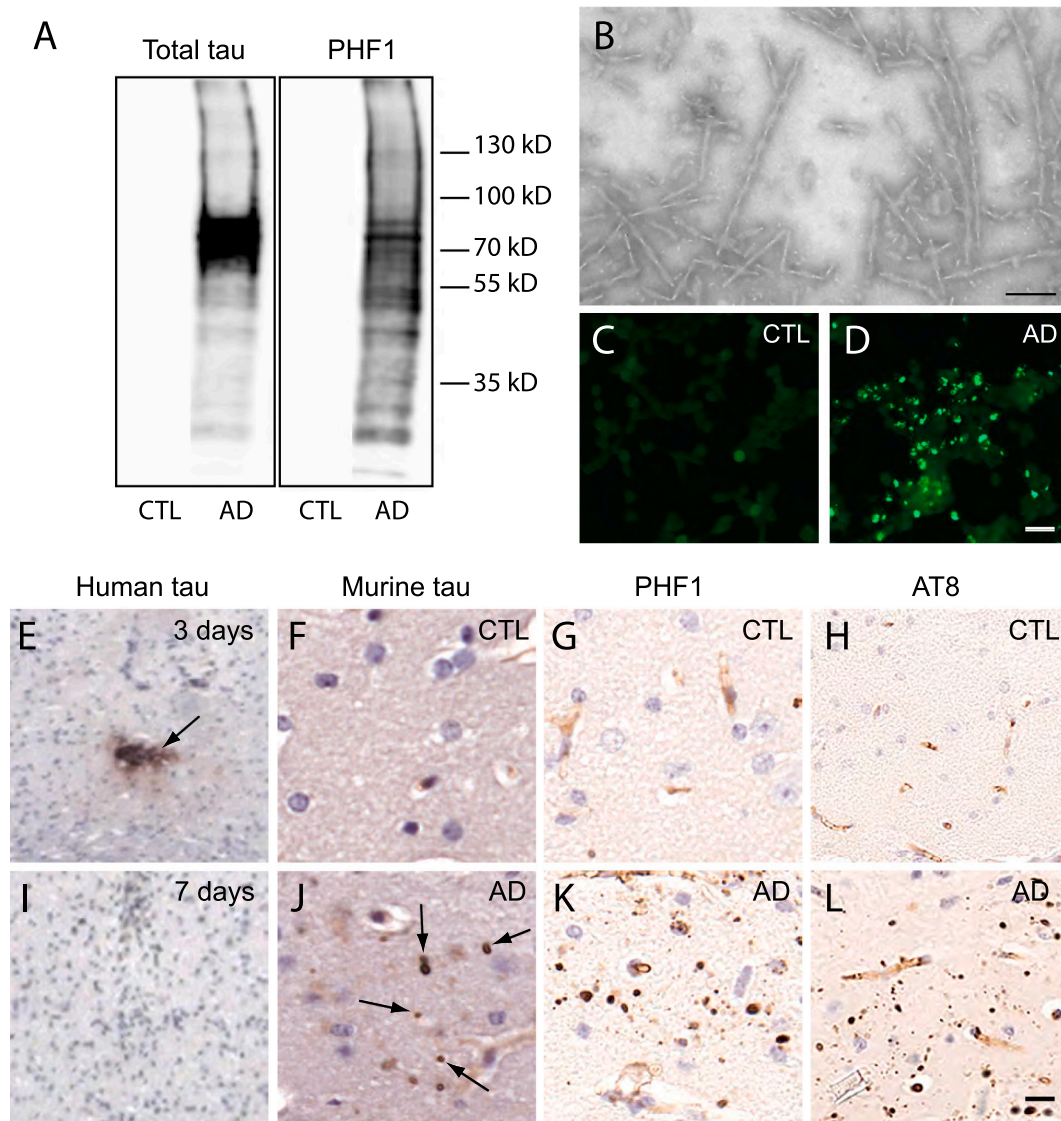


Fig. 2. PHF-tau proteins from AD sarkosyl fraction have the ability to induce the seeding of tau in cultured cells or in the brain of WT mice after stereotaxic injection. **A:** Western blotting of sarkosyl insoluble fraction from control (CTL) or Alzheimer's disease (AD) brains (PHF-tau) with anti-phosphotau antibody (PHF1) or total tau antibody (B19). Tau immunoreactivity was detected in sarkosyl fraction from AD brain but not in sarkosyl fraction from CTL brain. **B:** Sarkosyl insoluble fraction from AD brain contains paired helical filaments (PHF) observed by transmission electron microscopy. Scale bar: 50 nm. **C and D:** Detection of FRET signals in biosensor cells treated with CTL (C) or AD sarkosyl fractions. FRET signal is observed in AD treated cells (D) but absent in CTL treated cells (C). **E – L:** Immunolabelling on mouse brains intracerebrally injected by stereotaxy in the primary somatosensory cortex with sarkosyl fraction from CTL (F-H) or AD (E, I-L) sarkosyl fractions with anti-human tau (E and I), anti-murine tau (F and J), and with anti-phosphotau antibodies (PHF-1 in G and K, AT8 in H and L). Injected material was detected in the brain 3 days after injection (E) and has disappeared 7 days after injection (I). 3 months after injection, tau positive inclusions were observed in mice injected with AD fraction (J-L) but not in mice injected with CTL fraction (F-H). Slides were counterstained with Hematoxylin. Scale bar: 20 μ m.

from AD brain was confirmed by negative staining by electron microscopy (Fig. 2 B). The seeding ability of PHF-tau proteins in AD sarkosyl fraction was tested in the biosensor FRET assay cells (Fig. 2 C and D). We have observed a FRET signal in cells treated with AD sarkosyl fraction (Fig. 2 C) but not in cells treated with CTL sarkosyl fractions (Fig. 2 D) suggesting a seeding of recombinant tau by AD sarkosyl fraction in these cells. Moreover, we have analysed the seeding capacity of PHF-tau proteins after intracerebral injection in the somatosensory cortex of WT mice. We have detected human AD PHF-tau proteins (injected material) in the brain of WT mice 3 days after stereotaxic injection, but this material is not anymore detectable 7 days after the injection. 3 months after intracerebral injection of PHF-tau proteins, we have observed a seeding of murine tau in a highly phosphorylated state in WT mice (Fig. 2 J-L) whereas no seeding was observed after injection of CTL

sarkosyl fractions (Fig. 2 F-H). Tau pathology propagated on approximately 1.2 mm in the anteroposterior axis but also in the contralateral part of the brain by the corpus callosum indicating that our PHF-tau proteins have seeding and propagating properties as we previously described (Audouard et al., 2016; Vergara et al., 2019).

3.3. Detection of the Cholera Toxin subunit B in the visual pathway

To validate our intraocular injection technique, we have first injected the cholera toxin subunit B in the posterior vitreous chamber of WT mice (Fig. 3). As previously described (Angelucci et al., 1996), cholera toxin subunit B was detected 24 h after the injection, in the ganglion cell layer of the retina, in the geniculate nucleus and the superior colliculus of the contralateral side of the brain (Fig. 3C-J). We have also observed

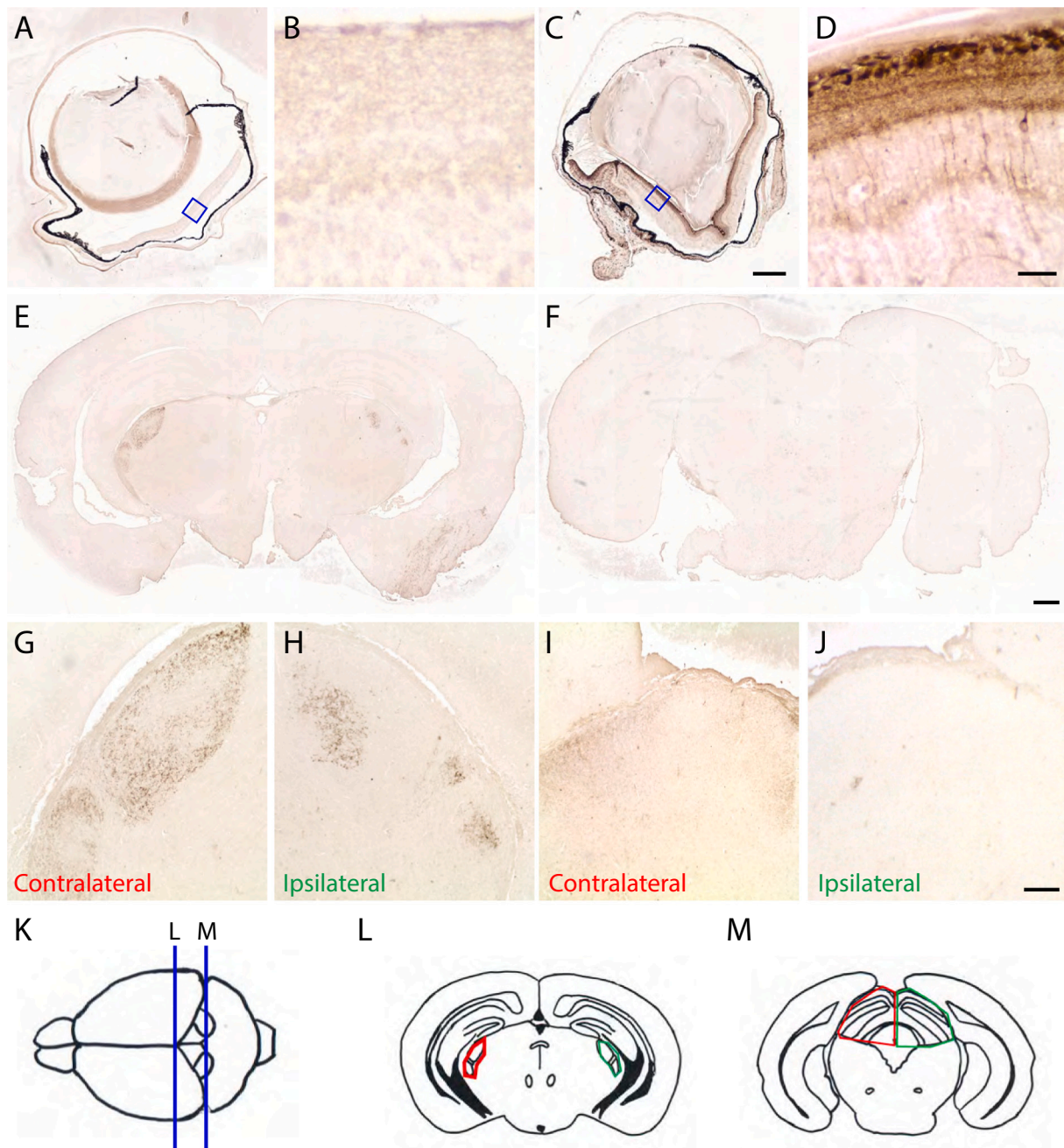


Fig. 3. Detection of the Cholera Toxin subunit B in the retina and in the brain of injected WT mice.

A – D: Immunolabelling of the eyes (A and C) of WT mice injected in the eye vitreous chamber with physiological serum (A) or subunit B of the Cholera Toxin (C) with anti-Cholera Toxin antibody. B and D are higher magnifications of a part of the retina corresponding to blue inset in A and C respectively. Scale bars: C: 200 μ m; D: 20 μ m.

E – J: Immunolabelling of the brain of WT mice injected in the eye vitreous chamber with subunit B of the Cholera Toxin (E and F) with anti-Cholera Toxin antibody. G, H, I and J are higher magnifications of the contralateral (G) and ipsilateral (H) lateral geniculate nucleus and of the contralateral (I) and ipsilateral (J) superior colliculus. Scale bars: F: 200 μ m; J: 40 μ m.

K – L: Schematic illustrations of coronal brain sections (antero-posterior localization shown in K) used to analyze the formation of tau pathology in the lateral geniculate nucleus (L) and the superior colliculus (M). The quantifications of tau pathology have been analysed in these brain areas delimited by a red line for the contralateral side and by a green line for the ipsilateral side of the brain.

cholera toxin positive axonal fibers in the geniculate nucleus of the ipsilateral side of the brain. Analysis in geniculate and superior colliculus regions have been further performed in brain areas as defined by red and green circles for contralateral (red) or ipsilateral (green) sides of the brain (Fig. 3 K and L).

3.4. PHF-tau proteins were internalized in the cytoplasm of the retinal ganglion cells

Localisation of PHF-tau proteins was examined in the eye at 10 min., 30 min., 1, 3, 6, 24 h and 5 days after the intravitreal injection in TauKO mice (Fig. 4). 3 h after the injection, PHF-tau proteins were detected in the posterior part of the vitreous in AD injected mice (Fig. 4 A and C) and

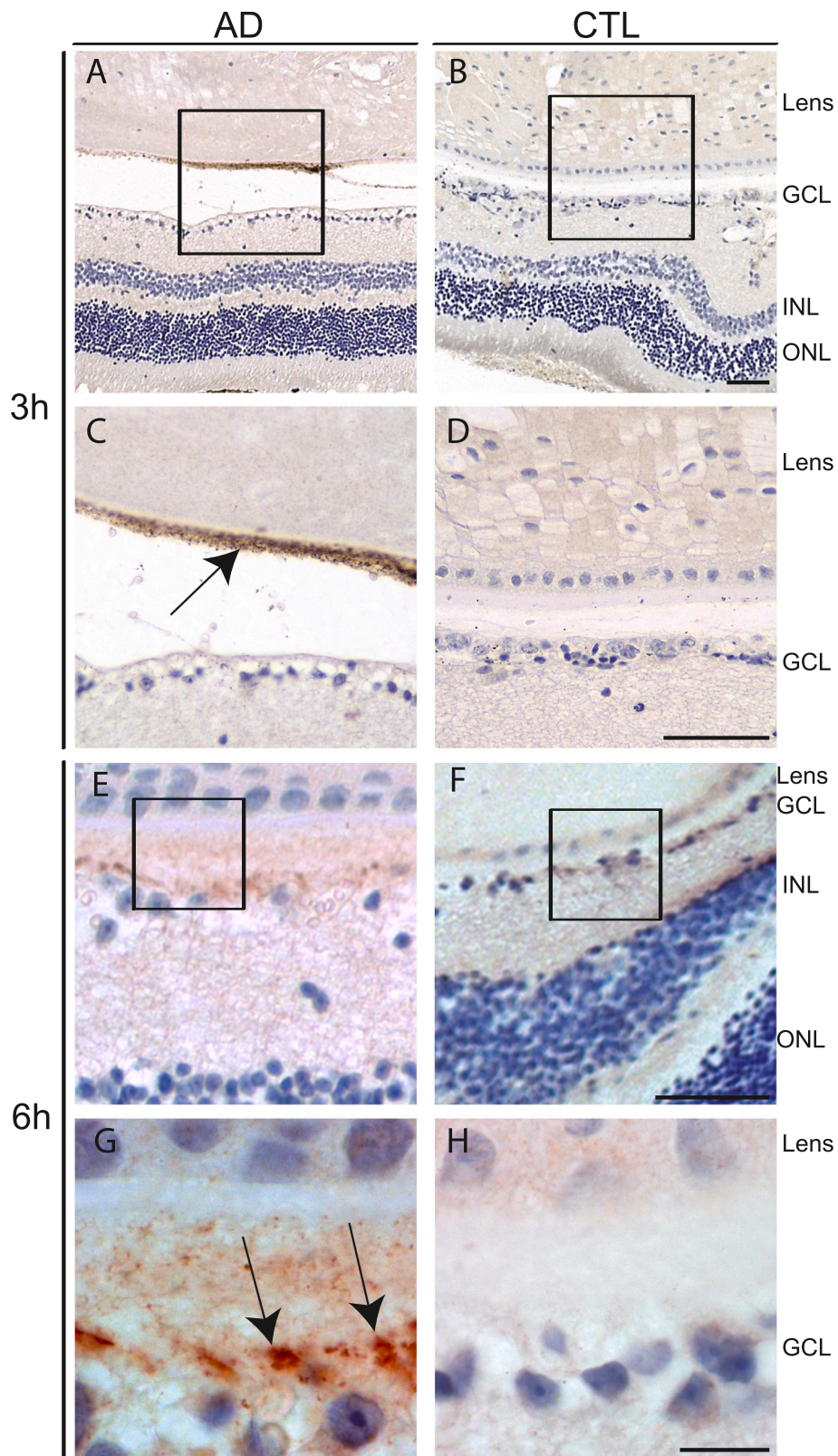


Fig. 4. PHF-tau proteins are detected in the ganglion cells 6 h after injection.

not in CTL injected mice (Fig. 4 B and D). 6 h after the injection, we have observed PHF-tau proteins in the cell bodies of ganglion cells (arrows in Fig. 4 G) of AD injected mice (Fig. 4 E and G) but not in CTL injected mice (Fig. 4 F and H). We next performed immunolabelling with AT8 or PHF1 antibodies to analyze the phosphorylation state of injected PHF-

tau proteins. These antibodies labelled PHF-tau proteins in the posterior part of the vitreous in AD injected mice 3 h after the injection but did not detect PHF-tau in the ganglion cells 6 h after the injection.

3.5. Analysis of the development of tau pathology in the visual pathway

To assess the propagation of tau pathology along the visual pathway after the internalisation of PHF-tau proteins in retinal ganglion cells, we have performed immunolabelling with antibodies recognizing phosphorylated tau on ser 396/404 (PHF-1 antibody) (Fig. 5 A, D, G, J and Fig. 6 A-E), on ser 202/thr 205 (AT8 antibody) (Fig. 5 B, E, H, K and Fig. 6 F-J) and recognizing conformational change (MC1 antibody) (Fig. 5 C, F, I, L and Fig. 6 K-O) on the brain of WT, hTau and Tg22 mice injected with CTL or AD sarkosyl fraction. We have analysed the presence of tau pathology along the visual pathway in the geniculate nucleus (Fig. 5) and in the superior colliculus (Fig. 6) of these injected mice after 6 months of incubation. Tau proteins have been detected in the neuropil in the geniculate nucleus like in other brain regions but a tau pathology was never observed in the geniculate nucleus of WT, hTau or Tg22 mice injected with AD or CTL sarkosyl fraction (Tg22 mice illustrated in

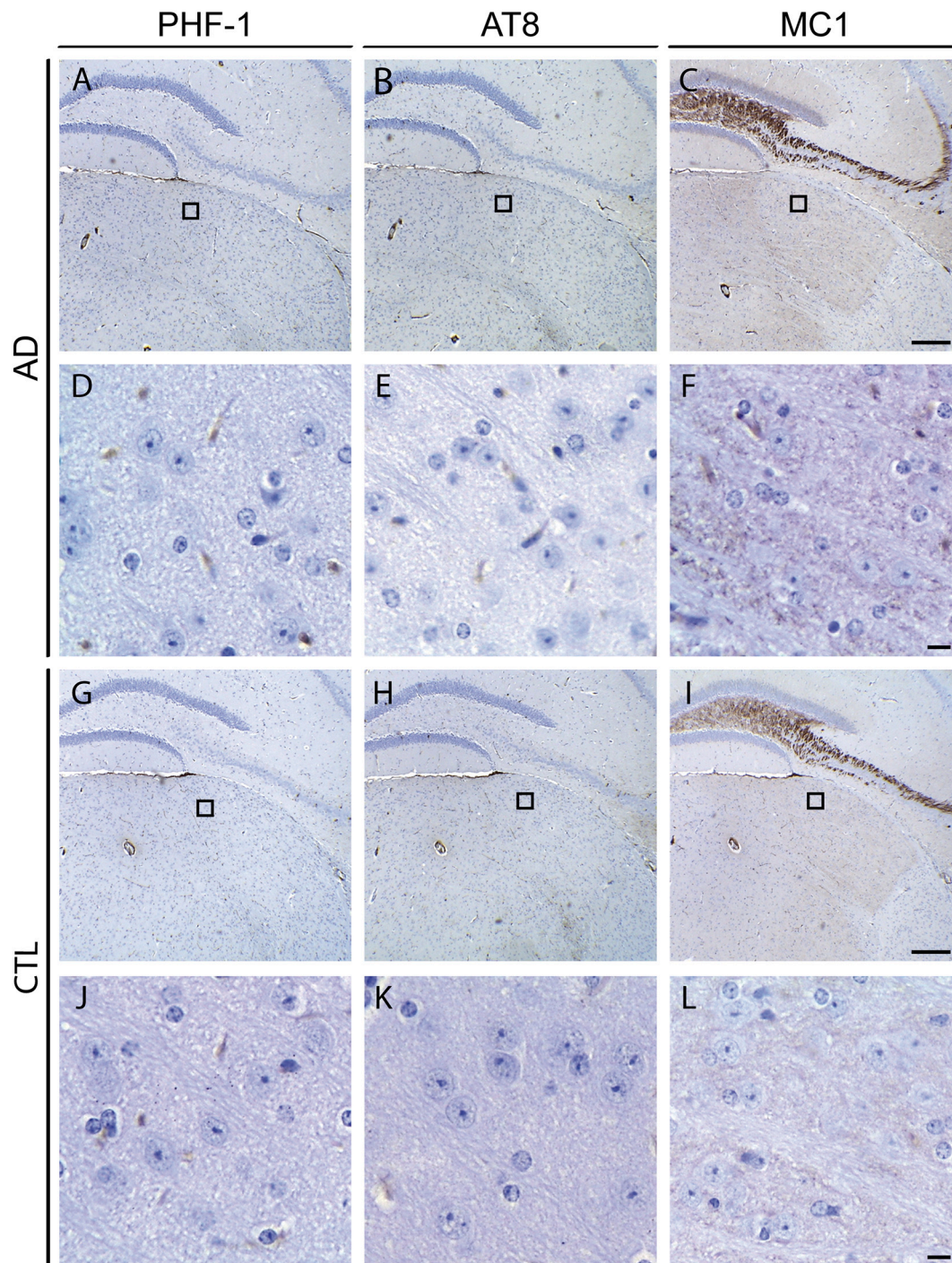


Fig. 5. Analysis of tau pathology spreading in the geniculate nucleus.

Immunolabelling of the geniculate nucleus of Tg22 mice with phosphotau antibodies (PHF-1 antibody recognizing phosphoserine 396/404 (A, D, G, J) or AT8 antibody raised against phosphoSer202/Thr205 (B, E, H, K) or with conformational antibody (MC1) (C, F, I, L) after intraocular injection of AD (A-F) or CTL (G-L) fractions. AD ($n = 5$) and CTL ($n = 4$). Pictures (D-F) and (J-L) are higher magnifications of the framed areas in pictures (A-C) and (G-I) respectively. Scale bars: I: 200 μm ; L: 10 μm .

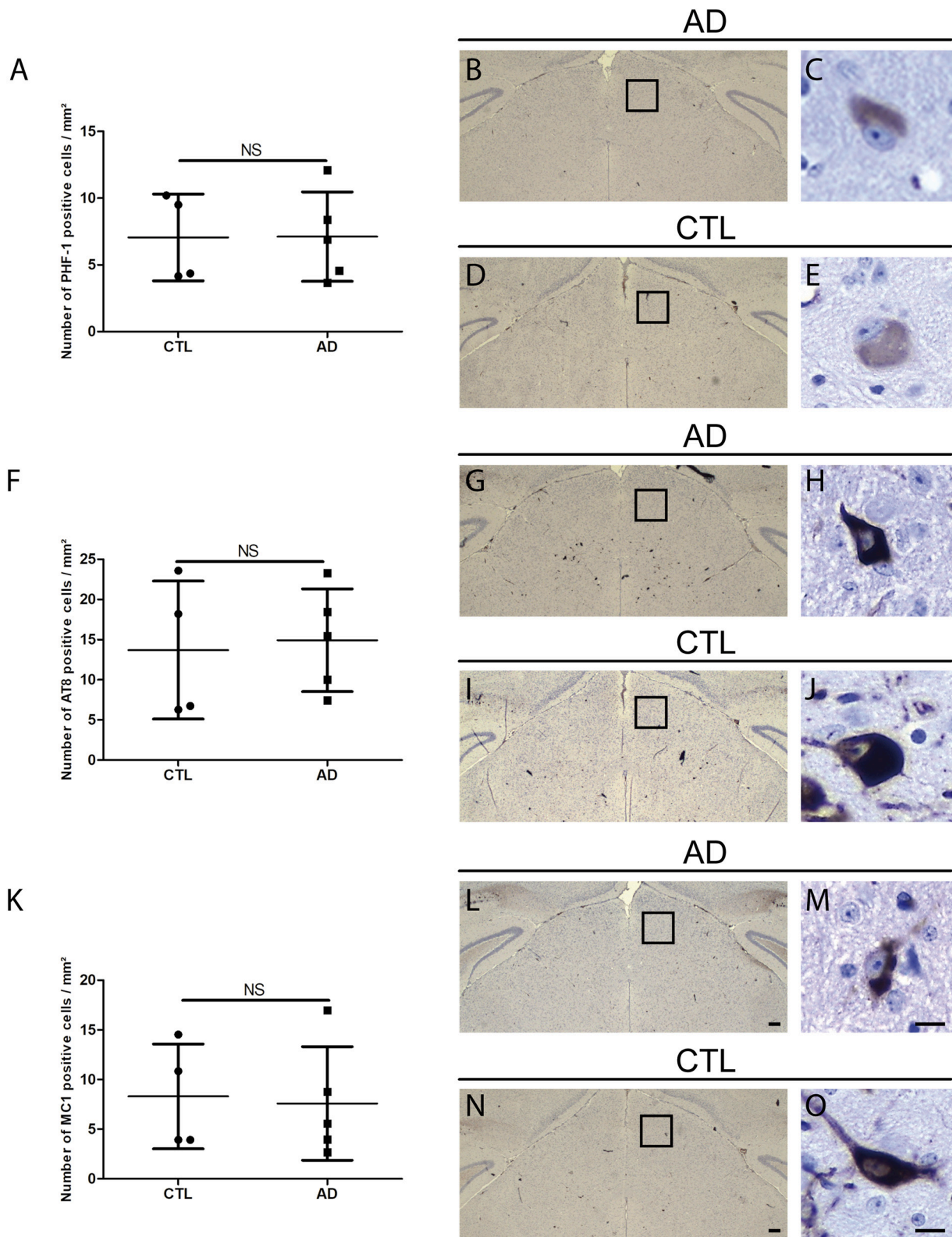


Fig. 6. Analysis of tau pathology spreading in the superior colliculus. Immunolabelling of the superior colliculus of Tg22 mice with phosphotau antibodies (PHF-1 antibody recognizing phosphoserines 396/404 (A-E) or AT8 antibody recognizing phosphoSer202/Thr205 (F-J)) or with conformational antibody (MC1) (K-O) after intraocular injection of AD (B-C, G-H, L-M) or CTL (D-E, I-J, N-O) fractions. Cells in (C,E,H,J,M,O) come from the framed areas in a part of the superior colliculus in pictures (B,D,G,I,L,N) respectively. The number of neurons showing phosphotau or conformational change of tau proteins is not significantly different between AD or CTL injected mice (AD (n = 5) and CTL (n = 4) (A: PHF-1 antibody, F: AT8 antibody, K: MC1 antibody). Two-tailed Mann-Whitney test. Scale bars: N: 200 μ m; O: 10 μ m.

Fig. 5). In the superior colliculus of Tg22 mice, a tau pathology was detected with PHF-1, AT8 and MC1 antibodies (Fig. 6C, E, H, J, M and O) but the quantification of tau pathology with the different antibodies did not show any differences between AD or CTL injected mice (PHF-1: $p = 0.8286$; AT8: $p = 0.6334$ and MC1: $p = 0.6965$) (Fig. 6 A, F and K).

4. Discussion

Alzheimer's disease is the most frequent cause of dementia representing a health challenge for our ageing societies. In this disease, intraneuronal lesions called neurofibrillary tangles are characterized by the misfolding and the accumulation of tau proteins in neurons leading to neuronal dysfunction and cognitive deficits. These lesions spread progressively between synaptically connected brain regions during the evolution of the disease. Previous studies have shown that the intracerebral injection of pathological tau proteins recruit and seed the aggregation of normal endogenous tau proteins suggesting that pathological tau proteins could share some common properties with prions (Clavaguera et al., 2013; Audouard et al., 2016; Vergara et al., 2019). It was previously observed that prions propagate in the retino-ectal pathway after corneal or sclera grafts in humans (Duffy et al., 1974; Heckmann et al., 1997; Mehta and Franks, 2002; Head et al., 2003; Head et al., 2005) or even after intraocular injection of prions in experimental models (Fraser, 1982). Pathological prion proteins have been observed in the plexiform layers of the retina of CJD patients (Head et al., 2003; Head et al., 2005) and intracerebral injection of eye homogenates from CJD subjects into non-human primates has shown transmission of the disease (Brown et al., 1994). To assess the ability of pathological tau (PHF-tau) to propagate tau seeding in the retino-ectal pathway we have analysed the formation and propagation of tau pathology along this pathway in several mice models expressing murine or human tau, after intraocular injection of PHF-tau isolated from AD brain.

In the retina, tau proteins have similar functions to those found in the brain such as stabilizing microtubules and regulating axonal transport (Ho et al., 2012) but are also implicated in axon development during retinal ganglion cells differentiation (Wang et al., 2000; Lieven et al., 2007) and in visual plasticity in adult mice (Rodriguez et al., 2020). Tau proteins are mainly expressed in a dephosphorylated form in all layers of the human retina (Löffler et al., 1995; Leger et al., 2011). In AD, tau proteins are hyperphosphorylated in all layers of the retina except the ONL (Löffler et al., 1995; Schön et al., 2012; Den Haan et al., 2018; Grimaldi et al., 2019) but never in a fibrillated (Den Haan et al., 2018) or an aggregated form (Schön et al., 2012). Moreover, the typical structures formed by tau proteins in the AD brain (tangles, neuritic plaques and neuropil threads) are not found in the retina (Den Haan et al., 2018).

We first validated our intraocular injection procedure using the cholera toxin subunit B that as expected (Angelucci et al., 1996) was rapidly transported along the retino-ectal pathway.

We observed the internalisation of injected PHF-tau into the retinal ganglion cells a few hours after intraocular injection. In a recent study using similar time points as us, a retinal uptake of fibrils made of truncated human K18 tau fragments after their intravitreal injection in WT mouse eyes was not observed (Veys et al., 2021). The discrepancy with our results showing an internalisation of PHF-tau in retinal ganglion cells could be explained by the nature of injected material, since Veys et al. injected fibrils composed of recombinant K18 whereas we injected native PHF-tau proteins isolated from AD brains. Our injected material exhibits many post-translational modifications found in AD such as conformational and phosphorylated epitopes which can play an important role in their ability, not only to form aggregates, but also to be internalized into cells (Alonso et al., 2001; Despres et al., 2017; Carlo-magno et al., 2021). For instance, tau proteins phosphorylated by glycogen synthase kinase-3beta were observed to be internalized into cortical cells ten times more easily than the low phosphorylated ones (Wauters et al., 2016). These observations suggest that the absence of

retinal uptake of K18 tau fragments could be due to the absence of phosphorylation, and potentially other post-translational modifications, of these recombinant peptides.

Despite the internalisation of PHF-tau in retinal ganglion cells, we did not observe aggregation of endogenous tau proteins expressed by these cells, either wild-type murine tau (WT mice), wild-type human tau (hTau mice), or aggregation prone human tau (THY-tau22 mice).

A previous study showed that the expression of human tau in mice significantly accelerates propagation of AD brain-derived pathological tau compared to mice expressing murine tau suggesting increased seeding abilities of human tau versus murine tau (Saito et al., 2019). We could however not detect tau aggregation in retinal ganglion cells even in our mice expressing human tau. The absence of tau seeding in the retinal ganglion cells could be due to the biochemical/conformational properties of the pathological fibrillar tau aggregates used in our study. However, the seeding ability of our PHF-tau fibrillar aggregates has been demonstrated in this study and previous ones (Audouard et al., 2016; Vergara et al., 2019) after intracerebral injection that induced aggregation of murine tau. Our results suggest rather that the absence of seeding in the retinal ganglion cells is not due to the absence of seeding activity of our injected PHF-tau fibrillar aggregates but is rather due to a resistance of these cells to develop a tau pathology. A previous study has shown that dephosphorylation of tau derived from AD brain reduces the seeding activity of tau (Wu et al., 2021). In our study, PHF-tau proteins internalized in ganglion cells are dephosphorylated for AT8 and PHF1 epitopes suggesting that phosphatases activity in ganglion cells could protect the cells against tau seeding. Indeed, in retina of AD patients, tau proteins accumulate in cell bodies of retinal ganglion cells (Schön et al., 2012; Den Haan et al., 2018) but these tau proteins are not aggregated supporting the hypothesis that these cells are resistant to induction of tau seeding.

Contrary to what has been observed for prions in Creutzfeldt-Jacob's disease, the presence of tau pathology has never been described in cornea or sclera of AD patients. However, studies in mice have shown the presence of phosphorylated tau in the cornea suggesting that corneal grafts could be at risk (Zhao et al., 2013; Li et al., 2022). Absence of transmission of AD after transplantation of corneal tissue has not been reported to our knowledge. Our comparative analysis of tau expression level in the eye and the brain, showed a significantly lower expression level of tau in the eye compared to the brain of the different mouse models used in this study; a concentration-dependent kinetic of tau aggregation could be a factor explaining the resistance of retinal ganglion cells to induction of tau seeding. Indeed, increasing the level of tau expression favours tau aggregation in transgenic models and in human tauopathies. Eg an increased level of tau expression due to MAPT gene duplication causes the formation of a tau pathology (Le Guennec et al., 2017).

Prion propagates rapidly (Gibbs Jr et al., 1994; Zobeley et al., 1999) but contrary to what has been observed for prions in previous studies, we did not observe a tau pathology propagation from the eye to the brain in our mice models even after 6 months of incubation. Tau pathology was not observed at the level of the two synaptic relays of the retino-ectal pathways, ie the geniculate nucleus and the superior colliculus in WT and htau mice. The absence of tau pathology propagation is not due to disturbances in the axonal transport in mice overexpressing tau proteins as it was shown that the absence or the overexpression of tau did not affect axonal transport in ganglion cells (Yuan et al., 2008). Tau pathology was present in these brain areas in THYtau-22 mice, but was not quantitatively different between mice injected with PHF-tau or control fractions, suggesting that this tau pathology is part of the phenotype of THY-tau 22 mice expressing an aggregation prone mutant tau under control of the Thy1.2 promoter.

We can not exclude that longer incubation times would lead to tau protein aggregation and propagation. Also, we cannot exclude that another form of pathological tau, such as tau oligomers, could be more efficient to induce tau aggregation and spreading in the visual pathway.

5. Conclusion

We evidenced for the first time that pathological tau proteins isolated from AD brains can enter into retinal ganglion cells after intraocular injection. We did not demonstrate a transmission of tau pathology to the brain after an ocular contamination in our mice models. We cannot exclude however that there is no risk of transmission by the retino-tectal pathway in human in whom longer incubation time should be possible, but our results suggest that eye surgery is not a major risk of transmission of tau pathology.

Immunolabelling with anti-human tau antibody of the eye of AD (A and C, E and G) or CTL (B and D, F and H) injected TauKO mice, 3 h (A-D) or 6 h (E-H) after the intraocular injection. 3 h after injection, PHF-tau proteins were detected near the posterior part of the lens (C) whereas this injected material was detected in the ganglion cells of the retina 6 h after the injection (G). Scale bars: B, D and F: 50 μ m; H: 10 μ m.

Funding

K. L. was supported by the Fund Defay, the Fund Van Buuren, the Rotary (Hope in head), the Fondation Recherche Alzheimer / Stichting Alzheimer Onderzoek (FRA/SAO 2018-0021, FRA/SAO 2021-0028) and the Génicot Fund. J.P.-B. was supported by grants from the Belgian Fonds de la Recherche Scientifique Médicale (T.0027.19), the Fund Aline (King Baudouin Foundation), the Fondation Recherche Alzheimer / Stichting Alzheimer Onderzoek (FRA/SAO 2019-0027) and the Génicot Fund.

Availability of data

All data generated or analysed during this study are included in this published article.

Ethics approval and consent to participate

Autopsies were carried out after written informed consent was obtained from family members. This study on postmortem brain tissues was performed in compliance and following approval of the Ethical Committee of the Medical School of the Free University of Brussels (ethical protocol number: P2009/015).

Ethics approval of animal usage

All studies on animals were performed in compliance and following approval of the Ethical committee for the care and use of laboratory animals of the Medical School of the Free University of Brussels (Authorization number: 599 N).

Consent for publication

Not applicable.

Arrive guidelines

This study is in accordance with ARRIVE guidelines.

Author statement

DFMA and LK conceived and planned the experiments. DFMA carried out the experiments. YZ, DDR, SV, AK contributed to sample preparation. BL provided Tg22 model. DFMA, LK, BJP contributed to the interpretation of the results. LK took the lead in writing the manuscript. All authors provided critical feedback and helped shape the research, analysis and manuscript.

Declaration of Competing Interest

The authors declare that they have no conflict of interests.

Data availability

Data will be made available on request.

Acknowledgements

We are very grateful to late Dr. Peter Davies for providing PHF-1 and MC1 antibodies.

References

- Alonso, A., Zaidi, T., Novak, M., Grundke-Iqbal, I., Iqbal, K., 2001. Hyperphosphorylation induces self-assembly of τ into tangles of paired helical filaments/straight filaments. *Proc. Natl. Acad. Sci. U. S. A.* 98 (12), 6923–6928.
- Ando, K., Leroy, K., Héraud, C., Yilmaz, Z., Authélet, M., Suain, V., De Decker, R., Brion, J.-P., 2011. Accelerated human mutant tau aggregation by knocking out murine tau in a transgenic mouse model. *Am. J. Pathol.* 178(2), 803–816. <https://doi.org/10.1016/j.ajpath.2010.10.034>.
- Andorfer, C., Kress, Y., Espinoza, M., De Silva, R., Tucker, K.L., Barde, Y.A., Duff, K., Davies, P., 2003. Hyperphosphorylation and aggregation of tau in mice expressing normal human tau isoforms. *J. Neurochem.* 86, 582–590.
- Angelucci, A., Clascá, F., Sur, M., 1996 Mar. Anterograde axonal tracing with the subunit B of cholera toxin: a highly sensitive immunohistochemical protocol for revealing fine axonal morphology in adult and neonatal brains. *J. Neurosci. Methods* 65 (1), 101–112.
- Audouard, E., Houben, S., Masaracchia, C., Yilmaz, Z., Suain, V., Authélet, M., De Decker, R., et al., 2016 Oct. High-molecular-weight paired helical filaments from Alzheimer brain induces seeding of wild-type mouse Tau into an argyrophilic 4R Tau pathology in vivo. *Am. J. Pathol.* 186 (10), 2709–2722. <https://doi.org/10.1016/j.ajpath.2016.06.008>.
- Braak, H., Braak, E., 1991. Neuropathological staging of Alzheimer-related changes. *Acta Neuropathol.* 82 (4), 239–259.
- Brion, J.P., Hanger, D.P., Bruce, M.T., Couck, A.M., Flament-Durand, J., Anderton, B.H., 1991a. Tau in Alzheimer neurofibrillary tangles. N- and C-terminal regions are differentially associated with paired helical filaments and the location of a putative abnormal phosphorylation site. *Biochem. J.* 273 (Pt 1), 127–133.
- Brion, J.P., Hanger, D.P., Couck, A.M., Anderton, B.H., 1991b. A68 proteins in Alzheimer's disease are composed of several tau isoforms in a phosphorylated state which affects their electrophoretic mobilities. *Biochem. J.* 279 (Pt 3), 831–836.
- Brown, P., Gibbs Jr., C.J., Rodgers-Johnson, P., Asher, D.M., Sulima, M.P., Bacote, A., Goldfarb, L.G., Gajdusek, D.C., 1994 May. Human spongiform encephalopathy: the National Institutes of Health series of 300 cases of experimentally transmitted disease. *Ann. Neurol.* 35 (5), 513–529. <https://doi.org/10.1002/ana.410350504>.
- Carlomagno, Y., Manne, S., DeTure, M., Prudencio, M., Zhang, Y.J., Hanna Al-Shaikh, R., Dummore, J.A., Daugherty, L.M., Song, Y., Castanedes-Casey, M., Lewis-Tuffin, L.J., Nicholson, K.A., Wszolek, Z.K., Dickson, D.W., Fitzpatrick, A.W.P., Petrucelli, L., Cook, C.N., 2021 Mar 16. The AD tau core spontaneously self-assembles and recruits full-length tau to filaments. *Cell Rep.* 34 (11), 108843 <https://doi.org/10.1016/j.celrep.2021.108843>.
- Clavaguera, F., Akatsu, H., Fraser, G., Crowther, R.A., Frank, S., Hench, J., Probst, A., et al., 2013 Jun 4. Brain homogenates from human tauopathies induce tau inclusions in mouse brain. *Proc. Natl. Acad. Sci. U. S. A.* 110 (23), 9535–9540. <https://doi.org/10.1073/pnas.1301175110>.
- Den Haan, J., Morrema, T.H.J., Verbraak, F.D., de Boer, J.F., Scheltens, P., Rozemuller, A.J., Bergen, A.A.B., Bouwman, F.H., Hoozemans, J.J., 2018 Dec 28. Amyloid-beta and phosphorylated tau in post-mortem Alzheimer's disease retinas. *Acta Neuropathol Commun.* 6 (1), 147. <https://doi.org/10.1186/s40478-018-0650-x>.
- Despres, C., Byrne, C., Qi, H., Cantrelle, F.X., Huvent, I., Chambraud, B., et al., 2017 Aug 22. Identification of the Tau phosphorylation pattern that drives its aggregation. *Proc. Natl. Acad. Sci. U. S. A.* 114 (34), 9080–9085.
- Duff, K., Knight, H., Refolo, L.M., Sanders, S., Yu, X., Picciano, M., Malester, B., Hutton, M., Adamson, J., Goedert, M., Burki, K., Davies, P., 2000. Characterization of pathology in transgenic mice over-expressing human genomic and cDNA tau transgenes. *Neurobiol. Dis.* 7, 87–98.
- Duffy, P., Wolf, J., Collins, G., DeVoe, A.G., Streeten, B., Cowen, D., 1974 Mar 21. Letter: possible person-to-person transmission of Creutzfeldt-Jakob disease. *N. Engl. J. Med.* 290 (12), 692–693.
- Fraser, H., 1982. Neuronal spread of scrapie agent and targeting of lesions within the retino-tectal pathway. *Nature* 295, 149–150.
- Frederick, C., Ando, K., Leroy, K., Héraud, C., Suain, V., Buée, L., Brion, J.P., 2015. Rapamycin ester analog CCI-779/Temsirolimus alleviates tau pathology and improves motor deficit in mutant tau transgenic mice. *J. Alzheimers Dis.* 44, 1145–1156. <https://doi.org/10.3233/JAD-142097>.
- Furman, J.L., Holmes, B.B., Diamond, M.I., 2015 Dec 8. Sensitive detection of proteopathic seeding activity with FRET flow cytometry. *J. Vis. Exp.* 106, e53205 <https://doi.org/10.3791/53205>.

- Gibbs Jr., C.J., Asher, D.M., Koblina, A., Amyx, H.L., Sulima, M.P., Gajdusek, D.C., 1994. Transmission of Creutzfeldt-Jakob disease to a chimpanzee by electrodes contaminated during neurosurgery. *J. Neurol. Neurosurg. Psychiatry* 57, 757–758.
- Gijs, M., Ramakers, I.H.G.B., Visser, P.J., Verhey, F.R.J., van de Waarenburg, M.P.H., Schalkwijk, C.G., Nuijts, R.M.M.A., Webers, C.A.B., 2021 Nov 22. Association of tear fluid amyloid and tau levels with disease severity and neurodegeneration. *Sci. Rep.* 11 (1), 22675. <https://doi.org/10.1038/s41598-021-01993-x>.
- Goedert, M., Jakes, R., Vanmechelen, E., 1995. Monoclonal antibody AT8 recognises tau protein phosphorylated at both serine 202 and threonine 205. *Neurosci. Lett.* 189, 167e169.
- Grimaldi, A., Pediconi, N., Oieni, F., Pizzarelli, R., Rosito, M., Giubettini, M., Santini, T., Limatola, C., Ruocco, G., Ragozzino, D., Di Angelantonio, S., 2019 Sep 4. Neuroinflammatory processes, A1 astrocyte activation and protein aggregation in the retina of Alzheimer's disease patients, possible biomarkers for early diagnosis. *Front. Neurosci.* (13), 925. <https://doi.org/10.3389/fnins.2019.00925>.
- Head, M.W., Northcott, V., Rennison, K., Ritchie, D., McCardle, L., Bunn, T.J., McLennan, N.F., Ironside, J.W., Tullio, A.B., Bonshek, R.E., 2003 Jan. Prion protein accumulation in eyes of patients with sporadic and variant Creutzfeldt-Jakob disease. *Invest. Ophthalmol. Vis. Sci.* 44 (1), 342–346.
- Head, M.W., Peden, A.H., Yull, H.M., Ritchie, D.L., Bonshek, R.E., Tullio, A.B., Ironside, J.W., 2005 Sep. Abnormal prion protein in the retina of the most commonly occurring subtype of sporadic Creutzfeldt-Jakob disease. *Br. J. Ophthalmol.* 89 (9), 1131–1133.
- Heckmann, J.G., Lang, C.J., Petruc, F., Druschky, A., Erb, C., Brown, P., Neundörfer, B., 1997 Sep. Transmission of Creutzfeldt-Jakob disease via a corneal transplant. *J. Neurol. Neurosurg. Psychiatry* 63 (3), 388–390.
- Ho, W.L., Leung, Y., Tsang, A.W., So, K.F., Chiu, K., Chang, R.C., 2012. Review: tauopathy in the retina and optic nerve: does it shadow pathological changes in the brain? *Mol. Vis.* 18, 2700–2710.
- Jicha, G.A., Bowser, R., Kazam, I.G., Davies, P., 1997. Alz-50 and MC-1, a new monoclonal antibody raised to paired helical filaments, recognize conformational epitopes on recombinant tau. *J. Neurosci. Res.* 48, 128–132.
- Le Guennec, K., Quenez, O., Nicolas, G., et al., 2017. 17q21.31 duplication causes prominent tau-related dementia with increased MAPT expression. *Mol. Psychiatry* 22, 1119–1125. <https://doi.org/10.1038/mp.2016.226>.
- Leger, F., Fernagut, P.O., Canron, M.H., Léoni, S., Vital, C., Tison, F., Bezard, E., Vital, A., 2011 Jan. Protein aggregation in the aging retina. *J. Neuropathol. Exp. Neurol.* 70 (1), 63–68. <https://doi.org/10.1097/NEN.0b013e31820376cc>.
- Leroy, K., Menu, R., Conreur, J.L., Dayanandan, R., Lovestone, S., Anderton, B.H., Brion, J.P., 2000. The function of the microtubule-associated protein tau is variably modulated by graded changes in glycogen synthase kinase-3beta activity. *FEBS Lett.* 465, 34–38.
- Li, S., Shi, S., Luo, B., Xia, F., Ha, Y., Merkley, K.H., Motamedi, M., Zhang, W., Liu, H., 2022 Feb. Tauopathy induces degeneration and impairs regeneration of sensory nerves in the cornea. *Exp. Eye Res.* 215, 108900 <https://doi.org/10.1016/j.exer.2021.108900>.
- Lieven, C.J., Millet, L.E., Hoegger, M.J., Levin, L.A., 2007 Nov. Induction of axon and dendrite formation during early RGC-5 cell differentiation. *Exp. Eye Res.* 85 (5), 678–683. <https://doi.org/10.1016/j.exer.2007.08.001>.
- Löffler, K.U., Edward, D.P., Tso, M.O., 1995 Jan. Immunoreactivity against tau, amyloid precursor protein, and beta-amyloid in the human retina. *Invest. Ophthalmol. Vis. Sci.* 36 (1), 24–31.
- Mehta, J.S., Franks, W.A., 2002. The sclera, the prion, and the ophthalmologist. *Br. J. Ophthalmol.* 86, 587–592.
- Mudher, A., Colin, M., Dujardin, S., Medina, M., Dewachter, I., Naini, S.M.A., Mandelkow, E.M., Mandelkow, E., Buee, L., Goedert, M., Brion, J.P., 2017. What is the evidence that tau pathology spreads through prion-like propagation? *Acta Neuropathol. Commun.* 5, 99.
- Otvos Jr., L., Feiner, L., Lang, E., Szendrei, G.I., Goedert, M., Lee, V.M., 1994. Monoclonal antibody PHF-1 recognizes tau protein phosphorylated at serine residues 396 and 404. *J. Neurosci. Res.* 39, 669–673.
- Rodriguez, L., Joly, S., Zine-Eddine, F., Mdzomba, J.B., Pernet, V., 2020 Nov. Tau modulates visual plasticity in adult and old mice. *Neurobiol. Aging* 95, 214–224. <https://doi.org/10.1016/j.neurobiolaging.2020.07.024>.
- Romau-Sanjurjo, D., Regueiro, U., López-López, M., Vázquez-Vázquez, L., Ouro, A., Lema, I., Sobrino, T., 2022. Alzheimer's disease seen through the eye: ocular alterations and neurodegeneration. *Int. J. Mol. Sci.* 23 (5):2486.
- Saito, T., Mihira, N., Matsuba, Y., Sasaguri, H., Hashimoto, S., Narasimhan, S., Zhang, B., Murayama, S., Higuchi, M., Lee, V., Trojanowski, J., Saido, T., 2019 Aug 23. Humanization of the entire murine MAPT gene provides a murine model of pathological human tau propagation. *J. Biol. Chem.* 294 (34), 12754–12765.
- Schindowski, K., Bretteville, A., Leroy, K., Bégard, S., Brion, J.P., Hamdane, M., Buée, L., 2006. Alzheimer's disease-like tau neuropathology leads to memory deficits and loss of functional synapses in a novel mutated tau transgenic mouse without any motor deficits. *Am. J. Pathol.* 169, 599–616.
- Schön, C., Hoffmann, N.A., Ochs, S.M., Burgold, S., Filser, S., Steinbach, S., Seeliger, M. W., Arzberger, T., Goedert, M., Kretschmar, H.A., Schmidt, B., Herms, J., 2012. Long-term in vivo imaging of fibrillar tau in the retina of P301S transgenic mice. *PLoS One* 7 (12), e53547. <https://doi.org/10.1371/journal.pone.0053547>.
- Stygelbout, V., Leroy, K., Pouillon, V., Ando, K., D'Amico, E., Jia, Y., Luo, H.R., Duyckaerts, C., Erneux, C., Schurmans, S., Brion, J.P., 2014. Inositol trisphosphate 3-kinase B is increased in human Alzheimer brain and exacerbates mouse Alzheimer pathology. *Brain* 137, 537–552. <https://doi.org/10.1093/brain/awt344>.
- Tucker, K.L., Meyer, M., Barde, Y.A., 2001. Neurotrophins are required for nerve growth during development. *Nat. Neurosci.* 4, 29–37.
- Vanden Dries, V., Stygelbout, V., Pierrot, N., Yilmaz, Z., Suain, V., De Decker, R., Buée, L., Octave, J.N., Brion, J.P., Leroy, K., 2017. Amyloid precursor protein reduction enhances the formation of neurofibrillary tangles in a mutant tau transgenic mouse model. *Neurobiol. Aging* 55, 202–212. <https://doi.org/10.1016/j.neurobiolaging.2017.03.031>.
- Vergara, C., Houben, S., Suain, V., Yilmaz, Z., De Decker, R., Vanden Dries, V., Boom, A., Mansour, S., Leroy, K., Ando, K., Brion, J.P., 2019 Mar. Amyloid-β pathology enhances pathological fibrillary tau seeding induced by Alzheimer PHF in vivo. *Acta Neuropathol.* 137 (3), 397–412. <https://doi.org/10.1007/s00401-018-1953-5>.
- Veys, L., Van Houcke, J., Aerts, J., Van Pottelberge, S., Mahieu, M., Coens, A., Melki, R., Moechars, D., De Muynck, L., De Groef, L., 2021 Jan. Absence of uptake and prion-like spreading of alpha-synuclein and tau after intravitreal injection of preformed fibrils. *Front. Aging Neurosci.* 15 (12) <https://doi.org/10.3389/fnagi.2020.614587>, 614587.
- Wang, S.W., Gan, L., Martin, S.E., Klein, W.H., 2000 Aug. Abnormal polarization and axon outgrowth in retinal ganglion cells lacking the POU-domain transcription factor Brn-3b. *Mol. Cell. Neurosci.* 16 (2), 141–156. <https://doi.org/10.1006/mcne.2000.0860>.
- Wauters, M., Wattiez, R., Ris, L., 2016. Internalization of the extracellular full-length tau inside Neuro2A and cortical cells is enhanced by phosphorylation. *Biomolecules* 6 (3), 36. <https://doi.org/10.3390/biom6030036>.
- Wu, R., Li, L., Shi, R., Zhou, Y., Jin, N., Gu, J., Tung, Y.C., Liu, F., Chu, D., 2021 May. Dephosphorylation passivates the seeding activity of oligomeric tau derived from Alzheimer's brain. *Front. Mol. Neurosci.* 13 (14) <https://doi.org/10.3389/fnmol.2021.631833>, 631833.
- Yuan, A., Kumar, A., Peterhoff, C., Duff, K., Nixon, R.A., 2008 Feb 13. Axonal transport rates in vivo are unaffected by tau deletion or overexpression in mice. *J. Neurosci.* 28 (7), 1682–1687. <https://doi.org/10.1523/JNEUROSCI.5242-07.2008>.
- Zhao, H., Chang, R., Che, H., Wang, J., Yang, L., Fang, W., Xia, Y., Li, N., Ma, Q., Wang, X., 2013 Sep 13. Hyperphosphorylation of tau protein by calpain regulation in retina of Alzheimer's disease transgenic mouse. *Neurosci. Lett.* (551), 12–16. <https://doi.org/10.1016/j.neulet.2013.06.026>.
- Zobeley, E., Flechsig, E., Cozzio, A., Enari, M., Weissmann, C., 1999. Infectivity of scrapie prions bound to a stainless steel surface. *Mol. Med.* 5, 240–243.